LUND UNIVERSITY

The Complement Inhibitor CD59 Regulates Insulin Secretion by Modulating Exocytotic Events.

Krus, Ulrika; King, Ben; Nagaraj, Vini; Gandasi, Nikhil R; Sjölander, Jonatan; Buda, Pawel; Garcia Vaz, Eliana; Gomez, Maria; Ottosson Laakso, Emilia; Storm, Petter; Fex, Malin; Vikman, Petter; Zhang, Enming; Barg, Sebastian; Blom, Anna; Renström, Erik

Link to publication

The complement inhibitor CD59 regulates insulin secretion by modulating exocytotic events

Ulrika Krus[1], Ben C. King[2], Vini Nagaraj[1], Nikhil R. Gandasi[3], Jonatan Sjölander[2], Pawel Buda[1], Eliana Garcia-Vaz[1], Maria F. Gomez[1], Emilia Ottosson–Laakso[1], Petter Storm[1], Malin Fex[1], Petter Vikman[1], Enming Zhang[1], Sebastian Barg[3], Anna M. Blom[2,†], Erik Renström[1,†]

† T*hese authors jointly directed this work*

[1]Lund University Diabetes Center, Department of Clinical Sciences Malmö, Lund University, SE-205 02 Malmö, Sweden

[2]Department of Laboratory Medicine Malmö, Lund University, SE-205 02 Malmö, Sweden

[3]Dept of Medical Cell Biology, Uppsala University, Box 571, SE-751 23 Uppsala, Sweden

Correspondence to: Erik Renström, Lund University, Dept. of Clinical Sciences, The Wallenberg Laboratory floor 3, S-205 02 Malmö, Sweden; Tel. +46 40 39 11 57; fax: +46 40 39 12 22; e-mail: erik.renstrom@med.lu.se and Anna Blom, Lund University, Dept. of Laboratory Medicine, The Wallenberg Laboratory floor 4, S-205 02 Malmö, Sweden. Tel. +46 40 33 82 33; fax: +46 40 33 70 43; e-mail: anna.blom@med.lu.se

RESEARCH HIGHLIGHTS

CD59 is highly expressed and localized intracellularly in pancreatic beta cells
CD59 is required for glucose- and depolarization-evoked insulin secretion
CD59 enables regulated interactions between exocytotic fusion proteins
CD59 expression is affected by glucose and diabetes status

SUMMARY

Type 2 diabetes is triggered by reduced insulin production, caused by genetic and

environmental factors such as inflammation originating from the innate immune system.

Complement proteins are a component of innate immunity and kill non-self cells by

perforating the plasma membrane, a reaction prevented by CD59.

Human pancreatic islets express CD59 at levels comparable to insulin. CD59 is primarily

known as a plasma membrane protein in membrane rafts, but most CD59 proteins in

pancreatic beta-cells is intracellular. Removing extracellular CD59 disrupts membrane rafts

and moderately stimulates insulin secretion, whereas silencing intracellular CD59 markedly

suppresses regulated secretion by exocytosis, as demonstrated by TIRF imaging. CD59

interacts with the exocytotic proteins VAMP2 and Syntaxin-1. CD59 expression is reduced by

glucose and in rodent diabetes models, but upregulated in human diabetic islets potentially

reflecting compensatory reactions. This unconventional action of CD59 broadens the

established view of innate immunity in type 2 diabetes.

INTRODUCTION

The innate immune system triggers tissue damage in autoimmune diseases (Diana et al., 2011)

but it may also be a central player in other types of human disease. For example, type 2

diabetes has been coined an autoinflammatory disease, in which dysregulated immunity

causes disturbances in insulin production in pancreatic beta-cells and signaling in target

tissues (Donath and Shoelson, 2011; Odegaard and Chawla, 2013). Innate immunity includes

the complement system with more than thirty proteins present in large quantities in the

circulation, and also locally in tissues. Complement represents a first line of defence against

invading pathogens and also aids removal of apoptotic and transformed cells (Ricklin et al.,

2010). Complement proteins are primarily produced in the liver, but there is extensive

2

evidence for local expression in peripheral tissues (Andoh et al., 1998; Passwell et al., 1990; Strainic et al., 2008).

Complement protein expression in pancreatic beta-cells and their interplay with insulin production and the secretion machinery remain largely unexplored. However, there are reports of high expression of the membrane-associated complement inhibitor CD59 in human pancreatic islets (Bennet et al., 2001). In addition, soluble glycated CD59 may be a potential biomarker for type 2 diabetes (Ghosh et al., 2013). CD59 is a glycosylphosphatidylinositol (GPI)-linked protein located in lipid rafts (Miwa et al., 2012), which are membrane domains highly enriched with cholesterol and sphingomyelins (Suzuki et al., 2012). Lipid rafts act as platforms which enhance cellular signalling (Reeves et al., 2012), and are also suggested to cluster exocytotic proteins and influence secretion of hormones (Lang, 2007). Here, we investigated the expression of complement genes in pancreatic islets, and detailed the impact of CD59 on insulin secretion. Our data demonstrate an unanticipated function of CD59 other than its classical role in complement-mediated cell lysis. This unconventional CD59 action is directed at the molecular machinery of beta-cell exocytosis and appears to be engaged during the development of type 2 diabetes.

RESULTS AND DISCUSSION

CD59 is the most highly expressed complement gene in pancreatic islets, with decreased islet expression in rodent diabetes models

First, we determined the expression of complement genes by microarray in human pancreatic islets from 112 donors. Of 32 investigated genes 21 were significantly expressed over background, which was defined as the average of all negative control probes. The gene showing the highest signal was the complement inhibitor CD59 (fig 1A). The spontaneously diabetic Goto-Kakizaki (GK) rat shares many hallmarks of human type 2 diabetes and

develops several of the late complications. Insulin secretion in GK rats is reduced from an early age and deteriorates as diabetes develops (Ostenson et al., 1993). Out of the nine significantly expressed genes in GK and healthy Wistar rat islets, CD59 differed with decreased expression in GK compared to Wistar islets (fig 1B). Average CD59 protein levels in islets and erythrocytes tended to decrease in GK (S1C-D). The decreased gene expression of CD59 in GK islets was also confirmed in two other rodent models of diabetes; the Akita mouse (Wang et al., 1999) and the BB-rat (Akesson et al., 2007); (fig 1C-D). To explore whether the decreased expression could be driven by high blood glucose, CD59 expression was investigated after high-glucose incubations. In clonal rat beta cells (fig 1E) as well as human islets (fig 1F), exposure to high glucose decreased CD59 expression. Immunostaining of rat pancreas revealed that CD59 was expressed both in the islets and in the surrounding exocrine tissue (fig 1G). In addition to the expected plasma membrane location, CD59 was also found to colocalize with insulin in beta-cells. The degree of colocalization increased when islets were incubated in high concentrations of glucose (fig 1H-I and S1E). The insulin colocalization is intriguing, since CD59 has previously only been regarded as a membrane protein found on the extracellular surface (Kim and Song, 2006; Kimberley et al., 2007; Suzuki et al., 2012). The intracellular expression and colocalization with insulin granules suggested to us that CD59 may have additional functions in the beta-cell.

Silencing of CD59 decreases insulin secretion by reducing the number of exocytotic events

The localization of CD59 to insulin granules made us hypothesize that reduced CD59 expression could impair insulin secretion. Consequently, we silenced CD59 by RNA interference in insulin-secreting rat INS-1 832/13 cells (Hohmeier et al., 2000). First, CD59 expression was verified in these cells, both on the plasma membrane and intracellularly (fig

2A). Silencing was verified by both Q-PCR (fig 2B) and flow cytometry (fig 2C and S2B), and had no effect on total insulin content (fig 2D). We then investigated the functional consequences of CD59 silencing. Insulin secretion was stimulated with three secretagogues acting at various stages of the stimulus-secretion coupling in beta-cells (16.7 mM glucose, 10 mM alpha-KIC, and 35 mM K^+) in order to pinpoint the functional stage of action. Glucose undergoes glycolysis prior to mitochondrial metabolism, alpha-KIC acts as a mitochondrial substrate, and depolarizing concentrations of K^+ bypass metabolism and directly activate the voltage-gated Ca^{2+} channels to trigger exocytosis. In the CD59-silenced cells, basal secretion was unaffected, whereas insulin secretion was strongly and equally reduced in response to all three secretagogues (60%, 66%, and 63% respectively; fig 2E). The effect of silencing CD59 on glucose-stimulated insulin secretion was confirmed using two other siRNAs (fig S2C) and also in glucagon-secreting alpha TC1-6 cells (S2D).

The similar decrease in secretion in response to all tested secretagogues suggests that the site of inhibition is distal to metabolism, and most likely directly affecting the exocytotic reaction. We therefore investigated this process using total internal reflection (TIRF) microscopy. To address whether silencing of CD59 affects the release kinetics from individual granules, INS-1 832/13 cells were co-transfected with the granule marker NPY-EGFP and siRNA against CD59 or control siRNA, and exocytosis stimulated by exposure to high K^+. Individual exocytotic events were seen as a rapid disappearance of individual granules, as shown in fig. 2F (control) and 2G (CD59 siRNA). Interestingly, 24 % of the events in control cells were preceded by a bright flash indicating fusion pore formation (Barg et al., 2002), which occurred more rarely (14 %) after CD59 silencing The latter effect was probably due to faster release kinetics, which we analysed by extracting the fluorescence time course of individual events (examples in fig 2H). We aligned the traces to the first significant change from baseline, taken as the moment of fusion pore opening. The aligned average of CD59

silenced cells decayed to zero faster than controls, indicating faster granule emptying upon exocytosis (fig 2I-J).

However, the most striking finding was the dramatic reduction in the number of detected exocytotic events in response to K^+ in CD59 silenced cells (2 events/cell vs. 11 in control cells). Normalized for the area of the cell's footprint this translates to 0.13 ± 0.02 $min^{-1}\mu m^{-2}$ in controls (6 cells with 63 events) compared to 0.01 ± 0.01 $min^{-1}\mu m^{-2}$ in CD59 silenced cells (11 cells with 22 events) (fig 2K-L). The same reduction was seen also when only analyzing events with preceding flashes (S2G). In summary, silencing of CD59 strongly reduced the number of exocytosis events, but accelerated the release kinetics of the individual events that did occur.

CD59 is important for lipid raft stability

The location of CD59 in lipid rafts and its use as a lipid raft marker suggest that it might be of importance for these structures. We therefore stained lipid rafts using the lipid raft component sphingomyelin, fluorescently labelled with Atto647N (Eggeling et al., 2009). Staining of islet cells from healthy Wistar rats and diabetic GK exhibited a clear difference in lipid raft appearance. The lipid raft structure in GK rat islets was disrupted and the overall staining intensity was significantly lower (fig 3A). A similar reduction in lipid raft staining was observed in INS-1 832/13 cells silenced for CD59 (fig 3B), as well as in CD59-silenced endothelial A549 cells (fig 3C). Collectively, these observations strongly support that CD59 plays an important role in stabilizing lipid rafts, which is not restricted to endocrine cells.

Removal of extracellular CD59 does not decrease insulin secretion

Phospholipase C strips the plasma membrane of GPI-linked proteins including CD59, leaving only the diacylglycerol anchor in the plasma membrane. As a complementary method for

CD59 removal we treated INS-1 832/13 cells with PLC, and verified the loss of cell surface

CD59 by flow cytometry. With 1U/ml PLC the extracellular CD59 signal was reduced to

background levels (fig 3D). PLC-treated cells and controls were then stimulated with glucose.

Remarkably, the effect on insulin secretion after PLC treatment bore little resemblance to the

effect of CD59 silencing by siRNA. First, basal insulin release at 2.8 mM glucose was

significantly increased. Secondly, insulin secretion evoked by high glucose (16.7 mM) was

unaffected by PLC treatment as compared to control cells (fig 3E). To further investigate the

specificity of the influence of CD59 on insulin secretion, we stably overexpressed an

alternative GPI-linked protein, Thy-1, in INS-1 832/13 cells (fig S3A). These cells were then

silenced for CD59 and assayed for insulin secretion (fig 3F; S3B). Thy-1 overexpression did

not rescue impaired insulin secretion from CD59 silenced cells. Collectively, these results

suggest the involvement of two distinct mechanisms whereby CD59 controls insulin

secretion: the extracellular pool of CD59 is responsible for stabilization of lipid rafts, and

disruption of lipid rafts results in increased basal secretion. By contrast, the intracellular pool

of CD59 that is colocalized with insulin, and is removed by siRNA knockdown, but not by

extracellular PLC, is important for stimulated insulin secretion and regulated exocytosis.

CD59 is responsible for establishing the VAMP2-syntaxin complex

We hypothesized that intracellular CD59 regulates exocytosis via interaction with the

exocytotic machinery. SNARE proteins (soluble N-ethylmaleimide-sensitive factor

attachment protein receptor) control insulin granule fusion with the plasma membrane. The

transmembrane protein syntaxin1A and the membrane-associated protein SNAP-25 are

predominantly associated with the plasma membrane, whereas VAMP2 is a vesicular

membrane protein (Gerber and Sudhof, 2002). Upon Ca^{2+} entry, the SNARE complex

changes conformation forcing the granule to fuse with the plasma membrane (Jahn et al.,

2003). Immunostainings suggested that CD59 colocalized with syntaxin1A and VAMP2 (fig 4A and B). To investigate the interactions with better spatial stringency, we used the Duolink *in situ* detection method. Paired species-specific secondary antibodies with unique DNA oligonucleotides (Proximity Ligation Assay (PLA) probes) were used. When the PLA probes are in close proximity (<40 nm), the DNA strands interact and the signal is amplified via rolling circle amplification using a polymerase, yielding distinct bright dots of fluorescence. Cells were incubated in 2.8 and 16.7 mM glucose and then stained with either CD59 + syntaxin1A or CD59 + VAMP2 antibodies linked with Duolink. CD59 interacted with both syntaxin1A and VAMP2, as demonstrated by the appearance of distinct dots (fig 4C). These interactions between CD59 and the exocytotic proteins increased significantly upon stimulation with glucose (fig 4D). Next, we investigated whether CD59 plays a role in establishing the exocytotic fusion complex. Hence, Duolink with syntaxin1A and VAMP2 antibodies was performed in cells silenced for CD59. In control cells, interactions between syntaxin and VAMP2 increased significantly in high glucose, as expected under conditions stimulating exocytosis. However, in the CD59-silenced cells, glucose stimulation failed to do so (fig 4E and S4A). Instead, these remained static at an intermediate level. Similar results were obtained when using high K^+ as stimulus (S4C). As control, no increased interaction between CD59 and the lipid raft marker flotillin was observed in 16.7 mM glucose (fig S4B). With ELISA, a similar increase in interactions between CD59 and VAMP2 or syntaxin1A was seen upon glucose stimulation (fig 4F). Further evidence of interactions was obtained by immunoprecipitation, where syntaxin1A bound both CD59 and VAMP2 (fig 4G). Interestingly, only one form of CD59 was detected in the eluate, suggesting that the effect may involve only a subpopulation of CD59. Thus, CD59 influences the SNARE pairing required for exocytosis. The intermediate state reached in the silenced cells indicates that the role of CD59 could be to assist in the break-up or recycling of the exocytotic core complex

post-fusion, and that in the absence of CD59, inactive complexes accumulate and hence new ones cannot be formed. A role for CD59 in dissociation of the exocytotic complex could also provide ideas for further studies on the increased kinetics of the individual exocytotic events that do occur in CD59 silenced cells (Fig 2I).

Concerning the role of CD59 during diabetes development, reduced islet expression was observed in three different rodent models under conditions not associated with changes in beta-cell mass, as well as after 24-h high-glucose treatment in rat clonal cells and human islets. However, human islet CD59 expression exhibited a paradoxical positive correlation to clinical glucose control of the donors (HbA1c levels; fig. S1A-B). A possible explanation to this is that this finding reflects the attempt of beta-cells at compensating for a deteriorating insulin output. In fact, a major lesson from global RNA sequencing endeavours is that expression in diabetic islets can be very different from those observed in the pre-diabetic state when the majority of gene expression changes are observed (Fadista, Mollet and Groop, personal communication). A broader knowledge of islet gene expression changes during diabetes will help to put the present findings into perspective.

In summary, this study demonstrates a previously unknown interaction between a component of the innate immune system and the molecular machinery of hormone secretion. We demonstrate that the complement inhibitor CD59 exerts unconventional effects other than its well-known suppression of the lytic membrane attack complex. First, CD59 appears to play a role in maintaining lipid raft stability in different cell types, which in beta-cells has consequences for basal insulin release rates. Second, CD59 facilitates recycling of exocytotic core proteins and in its absence this process is arrested. This work paves the way for further studies on the roles of CD59 and the complement system in lipid raft biology and in hormonal disorders such as type 2 diabetes.

MATERIALS AND METHODS

Human islets

Human islets were provided by the Nordic Network for Islet Transplantation, Uppsala University. All procedures were approved by the ethics committees at Uppsala and Lund Universities.

Animals

Wistar, GK and BB rats and Akita mice of age 5-13 weeks were used in this study. All procedures were approved by the local ethics review board at Lund University and the Malmö/Lund Animal Care and Use Committee.

Gene expression analysis

Microarray in human pancreatic islets

RNA isolation from human islets was performed using the AllPrep DNA/RNA Mini Kit (Qiagen). Concentration and purity was measured using a NanoDrop ND-1000 spectrophotometer (NanoDrop Technologies). The microarrays were performed following the Affymetrix standard protocol for Human Gene 1.0 ST whole transcript based assay. Data were summarised and normalised with the RMA analysis method using R. The expression microarray data have been made available at the GEO database with accession number GSE54279.

Quantitative PCR

RNA was extracted using RNEasy (Qiagen). Gene expression was measured by QPCR using TaqMan (AppliedBiosystems).

RNA sequencing

Total RNA was extracted from 55 islet donors and RNA-seq libraries were generated (TruSeq RNA sample preparation kit, Illumina) and sequenced on an Illumina HiSeq 2000 using paired-end chemistry and 100-bp cycles to an average depth of 32M read pairs/sample. Reads

were aligned to hg19 using STAR [REF1] and read count calculated by HTSeq-count [REF2] and normalized using trimmed mean of M-values.

Immunostainings

CD59, insulin and glucagon were visualized by indirect immunohisto-/cytochemistry in pancreatic sections from normal rats, dispersed INS-1 832/13 or primary rat islet cells by indirect immunocytochemistry.

siRNA transfection

siRNA transfection was performed using Dharmafect (Dharmacon) and 30 nM oligonucleotides.

Flow cytometry

Cellular CD59 levels were assessed using mouse anti-rat CD59 (AbD serotec), followed by a FITC-labeled anti-mouse secondary (DAKO). For intracellular staining, cells were fixed using Fix&Perm kit (ADG Bioresearch) and then permeabilized using 0.5% Tween-20. Insulin costaining was performed using 1:200 guinea pig anti-insulin serum (Euro Proxima) followed by 1:200 anti-guinea pig Cy5. Cells were analysed using the Cyflow Space flow cytometer (Partec).

Insulin secretion

INS1-832/13 cells were preincubated for 2 hours in 2.8 mM glucose and then stimulated with 2.8 or 16.7 mM glucose or 2.8 mM glucose combined with 10 mM $\square$-KIC or 35 mM K^+ for one hour.

TIRF microscopy

INS-1 832/13 cells were imaged using a custom-built total internal reflection (TIRF) microscope. Exocytotic events were analysed as detailed in the supplemental material file.

Duolink *in situ* detection

INS-1 832/13 cells were incubated with primary antibodies of antibodies of anti-CD59 (NordicBioSite, AbD serotec), anti-VAMP2 (Abcam) and anti-syntaxin 1A (SYSY) over night. Continuous staining protocol followed the instruction from Olink Bioscience.

ELISA

INS-1 832/13 cells were lysed after incubation for 24h in 2.8 or 16.7 mM glucose. Lysates were incubated for 1h in microtiter plates coated with anti-VAMP2 (SYSY), anti-syntaxin 1 (SYSY) or isotype control antibodies (Immunotools). CD59 was then detected with biotinylated mouse antibodies followed by streptavidin-HRP (R&D). Absorbance was measured at 490 nm.

Immunoprecipitation

INS-1 832/13 cells were incubated in 16.7 mM glucose for 24h. After lysis, an aliquot was saved as 'Input' sample. Remaining lysate was mixed with anti-syntaxin-1 (SYSY) or isotype control covalently bound to magnetic DynaBeads® (Invitrogen, Life Technologies, USA) and incubated over-night. Beads were extensively washed with lysis buffer and co-precipitated proteins eluted

Statistics

Group means were compared with Student's unpaired two tailed T-test when two groups were compared, and with One- way ANOVA when multiple groups were compared. The Bonferroni method was used in case of multiple comparisons. The level of significance was set at $P < 0.05$.

Detailed protocols appended in the supplemental file.

FIGURE LEGENDS

Figure 1: Expression of complement genes (A) Complement genes significantly expressed over background in expression microarrays of human pancreatic islets (n = 112). (B) Expression of complement genes in Wistar and GK rat islets; n =3, **P <0.01 (C) Expression of CD59 in diabetes resistant (DR) and diabetes prone (DP) BB-rat islets; n = 4 for each group; *P < 0.05. (D) CD59 expression in islets from diabetic Akita and control non-diabetic WT mice; n =5 for Akita and 7 for WT; *P < 0.05. (E) Expression of CD59 in INS-1 832/13 cells after culture in 2.8 or 16.7 mM glucose for 2-72h; n = 3, **P <0.01 and ***P < 0.001 (F) Expression of CD59 in human islets cultured for 24h in 5.5 or 18.9 mM glucose measured with RNA sequencing; n = 53, **P <0.01. (G). Localization of CD59 in a pancreatic rat islet; n = 3. (H) Colocalization of CD59 (red) and insulin (green) in permeabilized primary rat islet cells; n = 3 (I) Percent of colocalization after culture at 2.8 or 16.7 mM glucose for 1h. The bars on the left indicate the amount of CD59 colocalized with insulin, and the bars on the right show the amount of insulin colocalized with CD59. *P < 0.05. See also figure S1E. All values are means ± S.E.M. mRNA levels are related to HPRT in 1B , D and E and to HPRT and Pol2a in 1C.

Figure 2: Silencing of CD59 in INS-1 832/13 cells decreases insulin secretion and exocytosis (A) Expression of CD59 in unpermeabilized and permeabilized INS-1 832/13 cells; n = 3. CD59 is located in the plasma membrane as well as in the cytosol. (B) CD59 mRNA levels relative to HPRT in siRNA control cells and cells treated with siRNA against CD59, 48 h after transfection. Values are means ± S.E.M. for three independent experiments; **P <0.01. See also figure S2A. (C) CD59 Protein expression levels 72 h after silencing of CD59 analysed by flow cytometry. Expression levels are shown as mean fluorescent intensity (% of untreated cells). Values are means ± S.E.M for four independent experiments. **P <0.01. See

14

also figure S2B. (D) Insulin content in silenced cells does not differ from control cells. Values are means ± S.E.M for three independent experiments. (E) Insulin secretion in static incubations is decreased after silencing of CD59. After siRNA transfection (72 h), 832/13 clonal beta-cells were stimulated with 2.8 mM glucose (glc), 16.7 mM glucose, or 2.8 mM glucose combined with 10 mM □-KIC or 35 mM K$^+$ respectively, over 1 h. Values are means ± S.E.M. for 3 independent experiments. For glucose and □-KIC ***P < 0.001. For K$^+$ **P < 0.01. See also figure S2C. (F-G) Examples of single granule exocytosis events measured with TIRF microscopy for siCtrl (F) and siCD59 (G), frames are 100 ms apart. (H) Traces of granule fluorescence for the events in F-G; squares, siCD59 and circles, siCtrl. (I) Averages of all traces as in H aligned to the first frame different from baseline (indicated by asterisks in F-G). (J) decay time and (K-L) Cumulative number of events per area detected in siCtrl and siCD59 cells and event frequency as defined in the text. The data are derived from 63 events detected in 6 independent experiments (cells) for siCtrl and 22 events in 11 cells for siCD59. See also figure S2E-G.

Figure 3: Extracellular CD59 in lipid rafts and insulin secretion

(A) Staining of lipid rafts in Wistar and GK rat islet cells reveals a significant lower mean intensity of lipid raft staining in the GK rat; n =3, *P < 0.05. (B) Silencing of CD59 in INS-1 832/13 cells decreases the amount of lipid rafts; n = 4, *P <0.05. (C) Silencing of CD59 in endothelial A549 cells exhibits the same decrease of lipid rafts as in beta cells, and proves the effect to be general and not specific for islet cells; n = 4, *P <0.05) Values are means and SEM for 3-4 independent experiments for all lipid raft stainings. (D) Treatment with PLC strips the plasma membrane of GPI-linked proteins, including CD59. Analyses with flow cytometry showed that 1 U/ml of PLC removes all extracellular CD59 from INS-1 832/13 cells; n = 3. Horizontal line, background fluorescence (isotype ctrl). (E) Insulin secretion in

INS-1 832/13 cells treated with PLC (1U/ml). The effect on insulin secretion when extracellular CD59 is removed does not mimic the effect of CD59 silencing; n =5,*P < 0.05.

(F) INS-1 832/13 cells stably overexpressing the GPI-linked protein Thy-1 were silenced for CD59 72h prior to insulin secretion. Thy-1 overexpression did not rescue the decreased insulin secretion caused by CD59 silencing; n = 4, **P < 0.01. Values are means and SEM for three to five independent experiments. See also figure S3.

Figure 4: CD59 is necessary for VAMP2 and Syntaxin 1A colocalization

(A) CD59 colocalizes with VAMP2; n = 3. (B) CD59 colocalizes with Syntaxin 1A; n = 3.

(C) Colocalization of CD59 with VAMP 2 and Syntaxin 1A using Olink PLA probes. A flouorescent dot is generated when two antibodies are closer than 40 nM. See also figure S4A.

(D) Quantification of Olink colocalization. Colocalization of CD59 and VAMP2 as well as CD59 and Syntaxin 1A increases in high concentrations of glucose. (E) Quantification of Olink colocalization of VAMP2 and Syntaxin 1A in cells where CD59 is silenced. In control cells, colocalization increases in presence of high glucose concentrations, whereas in the silenced cells, there is no response to high glucose. Values are means and SEM for three independent experiments, ***P < 0.001. See also figure S4B. (F) Binding of CD59 to VAMP2 and Syntaxin 1A in INS-1 832/13 cells measured with ELISA; n =4 ***P < 0.001.

(G) Immunoprecipitation with Syntaxin 1A antibodies in INS-1 832/13 cells. Both VAMP2 and CD59 were co-precipitated.

References

Akesson, L., Hawkins, T., Jensen, R., Fuller, J.M., Breslow, N.E., and Lernmark, A. (2007). Decreased core temperature and increased beta(3)-adrenergic sensitivity in diabetes-prone BB rats. Diabetes technology & therapeutics *9*, 354-362.
Andoh, A., Fujiyama, Y., Sakumoto, H., Uchihara, H., Kimura, T., Koyama, S., and Bamba, T. (1998). Detection of complement C3 and factor B gene expression in normal colorectal mucosa, adenomas and carcinomas. Clin Exp Immunol *111*, 477-483.

Barg, S., Olofsson, C.S., Schriever-Abeln, J., Wendt, A., Gebre-Medhin, S., Renstrom, E., and Rorsman, P. (2002). Delay between fusion pore opening and peptide release from large dense-core vesicles in neuroendocrine cells. Neuron *33*, 287-299.

Bennet, W., Bjorkland, A., Sundberg, B., Brandhorst, D., Brendel, M.D., Richards, A., White, D.J., Nilsson, B., Groth, C.G., and Korsgren, O. (2001). Expression of complement regulatory proteins on islets of Langerhans: a comparison between human islets and islets isolated from normal and hDAF transgenic pigs. Transplantation *72*, 312-319.

Diana, J., Gahzarian, L., Simoni, Y., and Lehuen, A. (2011). Innate immunity in type 1 diabetes. Discov Med *11*, 513-520.

Donath, M.Y., and Shoelson, S.E. (2011). Type 2 diabetes as an inflammatory disease. Nat Rev Immunol *11*, 98-107.

Eggeling, C., Ringemann, C., Medda, R., Schwarzmann, G., Sandhoff, K., Polyakova, S., Belov, V.N., Hein, B., von Middendorff, C., Schonle, A., et al. (2009). Direct observation of the nanoscale dynamics of membrane lipids in a living cell. Nature *457*, 1159-1162.

Gerber, S.H., and Sudhof, T.C. (2002). Molecular determinants of regulated exocytosis. Diabetes *51 Suppl 1*, S3-11.

Ghosh, P., Sahoo, R., Vaidya, A., Cantel, S., Kavishwar, A., Goldfine, A., Herring, N., Bry, L., Chorev, M., and Halperin, J.A. (2013). A specific and sensitive assay for blood levels of glycated CD59: A novel biomarker for diabetes. Am J Hematol.

Hohmeier, H.E., Mulder, H., Chen, G., Henkel-Rieger, R., Prentki, M., and Newgard, C.B. (2000). Isolation of INS-1-derived cell lines with robust ATP-sensitive K+ channel-dependent and -independent glucose-stimulated insulin secretion. Diabetes *49*, 424-430.

Jahn, R., Lang, T., and Sudhof, T.C. (2003). Membrane fusion. Cell *112*, 519-533.

Kim, D.D., and Song, W.C. (2006). Membrane complement regulatory proteins. Clin Immunol *118*, 127-136.

Kimberley, F.C., Sivasankar, B., and Paul Morgan, B. (2007). Alternative roles for CD59. Mol Immunol *44*, 73-81.

Lang, T. (2007). SNARE proteins and 'membrane rafts'. J Physiol *585*, 693-698.

Miwa, T., Zhou, L., Maldonado, M.A., Madaio, M.P., Eisenberg, R.A., and Song, W.C. (2012). Absence of CD59 exacerbates systemic autoimmunity in MRL/lpr mice. J Immunol *189*, 5434-5441.

Odegaard, J.I., and Chawla, A. (2013). Pleiotropic actions of insulin resistance and inflammation in metabolic homeostasis. Science *339*, 172-177.

Ostenson, C.G., Khan, A., Abdel-Halim, S.M., Guenifi, A., Suzuki, K., Goto, Y., and Efendic, S. (1993). Abnormal insulin secretion and glucose metabolism in pancreatic islets from the spontaneously diabetic GK rat. Diabetologia *36*, 3-8.

Passwell, J.H., Schreiner, G.F., Wetsel, R.A., and Colten, H.R. (1990). Complement gene expression in hepatic and extrahepatic tissues of NZB and NZB x W (F1) mouse strains. Immunology *71*, 290-294.

Reeves, V.L., Thomas, C.M., and Smart, E.J. (2012). Lipid rafts, caveolae and GPI-linked proteins. Adv Exp Med Biol *729*, 3-13.

Ricklin, D., Hajishengallis, G., Yang, K., and Lambris, J.D. (2010). Complement: a key system for immune surveillance and homeostasis. Nat Immunol *11*, 785-797.

Strainic, M.G., Liu, J., Huang, D., An, F., Lalli, P.N., Muqim, N., Shapiro, V.S., Dubyak, G.R., Heeger, P.S., and Medof, M.E. (2008). Locally produced complement fragments C5a and C3a provide both costimulatory and survival signals to naive CD4+ T cells. Immunity *28*, 425-435.

Suzuki, K.G., Kasai, R.S., Hirosawa, K.M., Nemoto, Y.L., Ishibashi, M., Miwa, Y., Fujiwara, T.K., and Kusumi, A. (2012). Transient GPI-anchored protein homodimers are units for raft organization and function. Nat Chem Biol.

Wang, J., Takeuchi, T., Tanaka, S., Kubo, S.K., Kayo, T., Lu, D., Takata, K., Koizumi, A., and Izumi, T. (1999). A mutation in the insulin 2 gene induces diabetes with severe pancreatic beta-cell dysfunction in the Mody mouse. The Journal of clinical investigation *103*, 27-37.
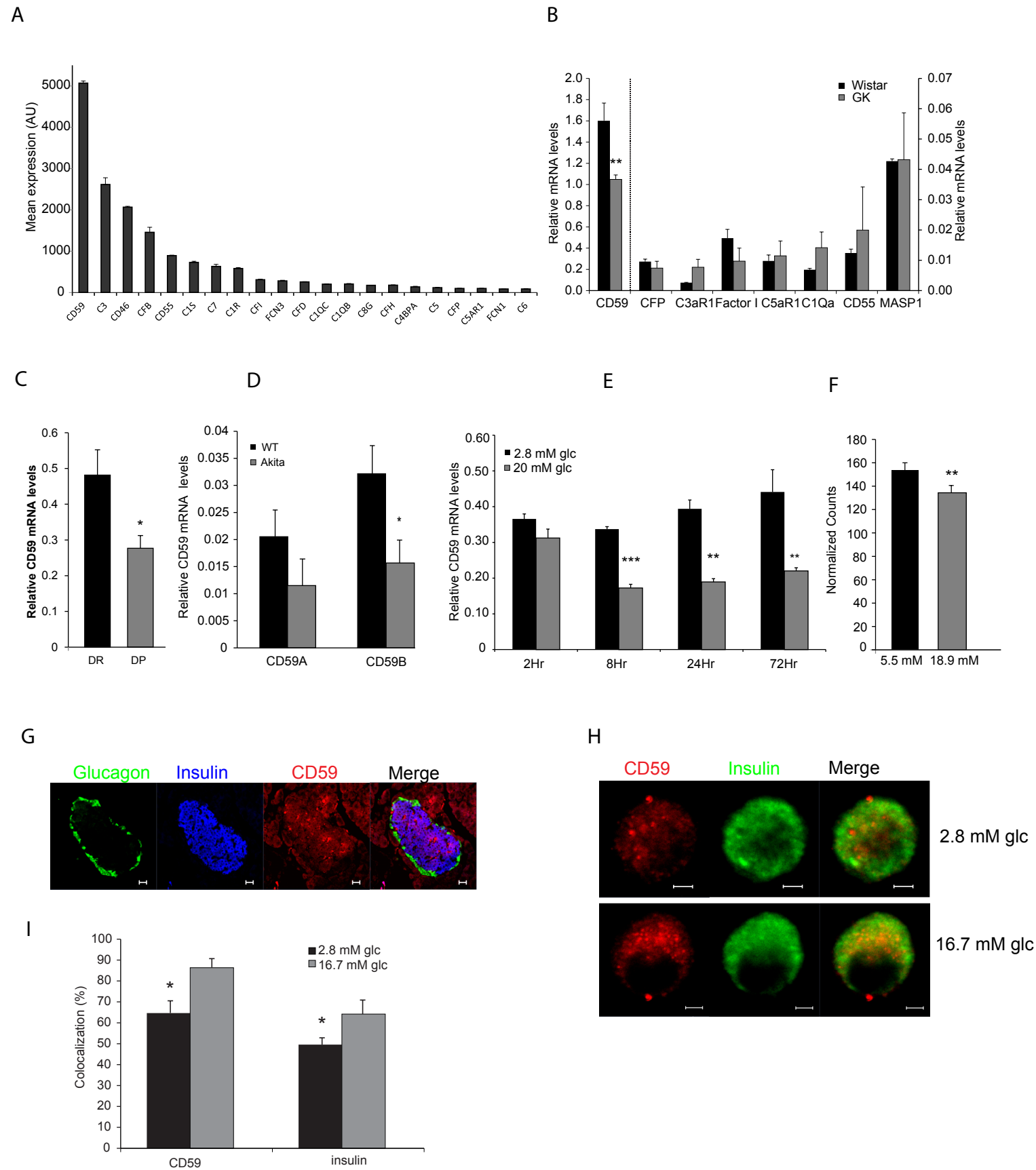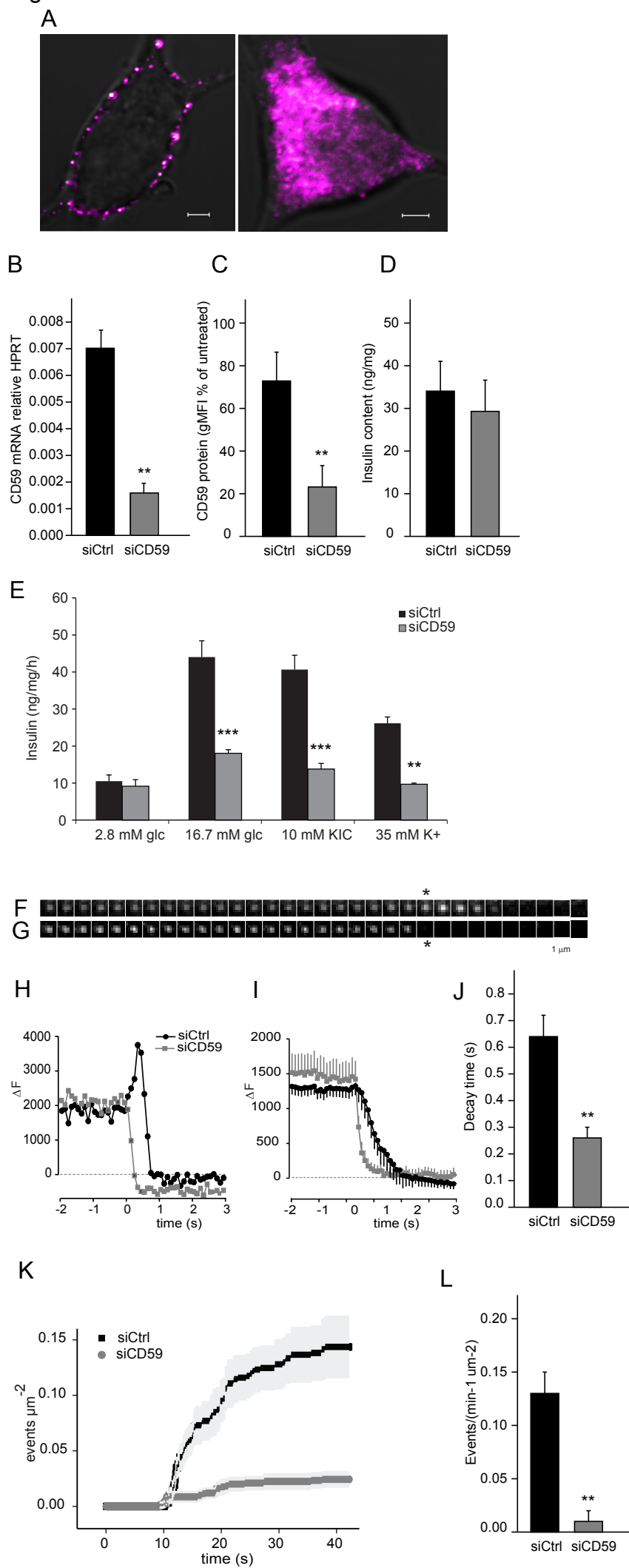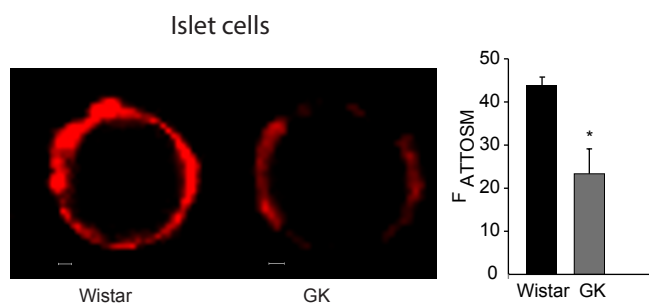
Figure 1
Figure 1

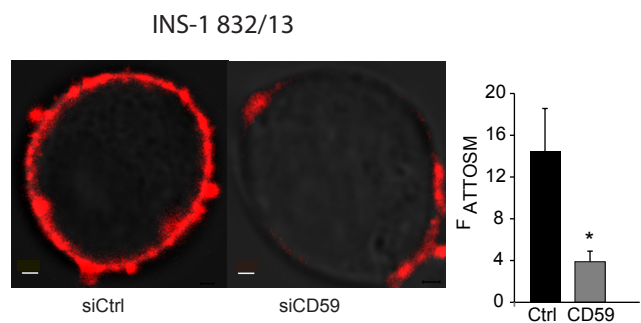Figure 2

A

B

C

D

E

F

G

H

I

J

K

L

Figure 3

Figure 3

A

Islet cells

Wistar   GK

B

INS-1 832/13

siCtrl   siCD59

C

A549

siCtrl   siCD59

D

E

F

Thy-1 transfected
INS-1 832/13 cells
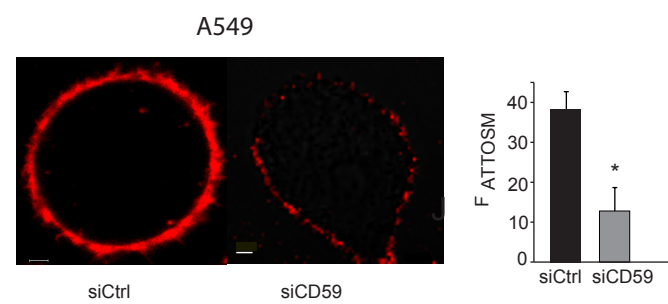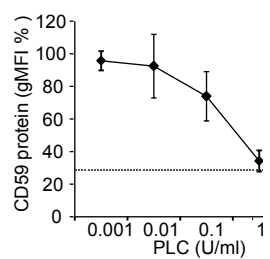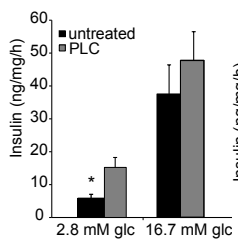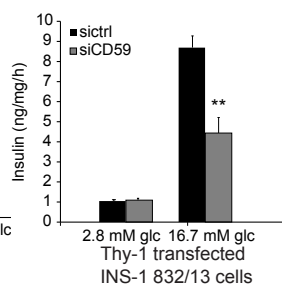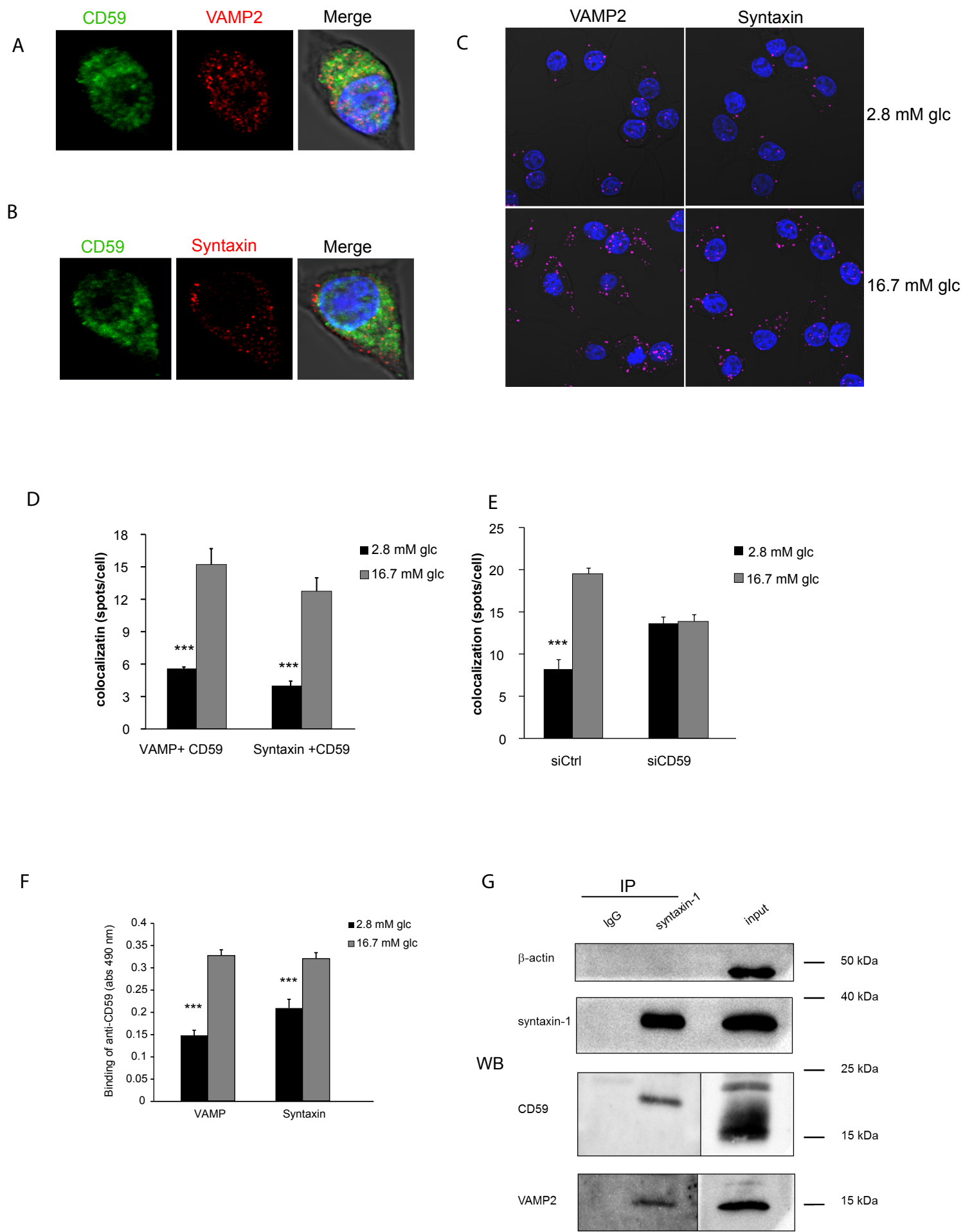
Figure 4

SUPPLEMENTAL FIGURES Krus et al. *The complement inhibitor CD59…*

A

B

C

D

E
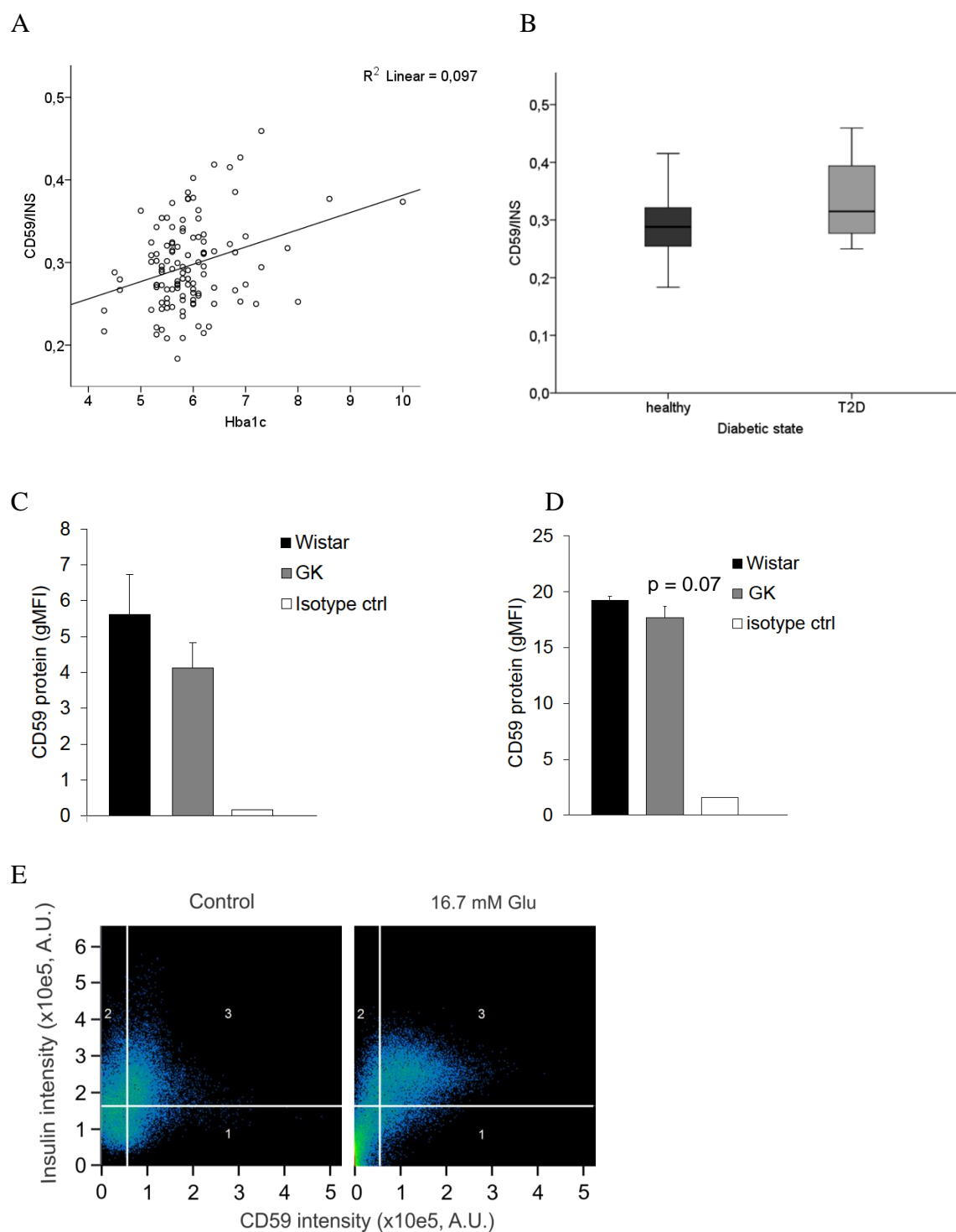
Figure S1: Expression patterns of CD59 in rat and human, related to figure 1

Expression of CD59 was assessed in 112 healthy and 16 diabetic individuals. (A) Expression
was positively associated with Hba1c **$P < 0.01$, and (B) significantly increased in the
diabetic individuals *$P < 0.05$. (C) CD59 protein levels on erythrocytes as well as on islets
(D) were compared between Wistar and GK rats. In both tissues, there was a tendency

1

towards a decrease in the GK rats, although not significant. Values are mean and SEM for 2-4 experiments. (E) Colocalization analysis of figure 1H. Analysis was performed using a ZEN2009 software based on Pearson's coefficient analysis which recognizes the colocalized pair by comparison pixel by pixel intensity. As a result form the analysis, the number 0 (%) indicates no colocalization and 100 means fully colocalized pair of pixels in a region of interest.
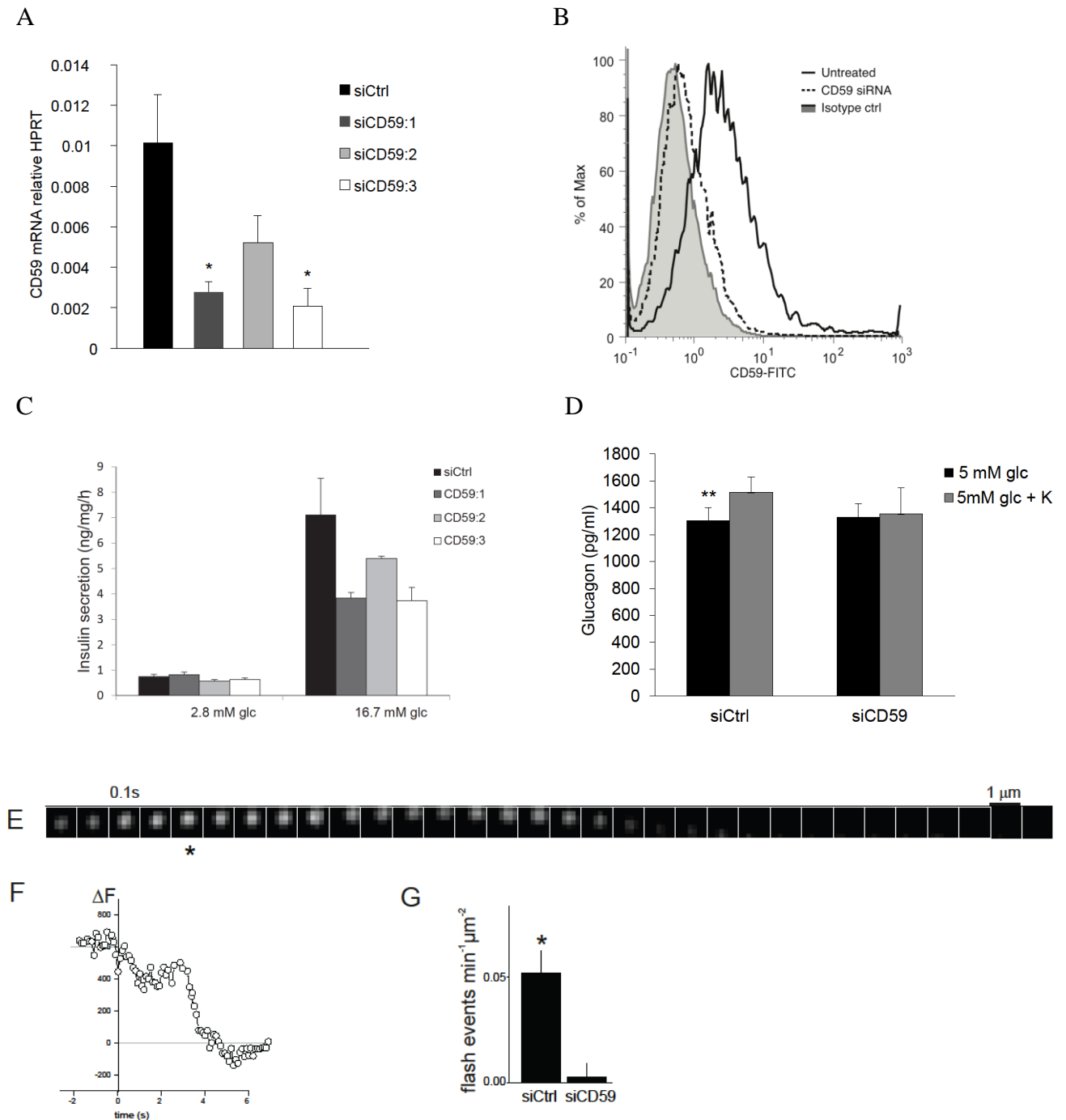
A

B

C

D

E

F

G

Figure S2: Efficiency of CD59 silencing and its effects on insulin and glucagon release, related to figure 2

(A) To validate the siRNA effect, we tested three different siRNAs against CD59. siCD59:3 had the strongest silencing effect and is the one used throughout the study. siCD59:1 had a

slightly weaker effect, whereas siCD59:2 had a low effect. Values are means and SEM for three independent experiments; * P < 0.05 for siRNA 1 and 3 vs. siCtrl. (B) FACS histograms of cells silenced with siCD59, siRNA controls and isotype control show efficient inhibition of expression in the whole population of silenced cells. (C) Insulin secretion after silencing CD59 with all three siRNAs. Insulin secretion was equally decreased with siCD59:1 and siCD59:3, but not with siCD59:2. This is consistent with the effect seen on mRNA level, where siCD59:2 did not silence as efficiently as the other two. Values are means and SEM for two independent experiments. (D) The mouse alpha cell line alphaTC1-6 was silenced for CD59 A and subsequently stimulated with 5 mM glucose or 5 mM glucose + 70 mM K^+. Glucagon secretion was significantly increased by K^+ in the control cells, whereas no effect was seen in cells silenced for CD59A. Values are means and SEM for three independent experiments. p <0.01 with paired Students t-test. (E-F) TIRF microscopy showing granule undocking to the granule interior. (G) Analysis of exocytosis frequency using flashing events only.

A

B
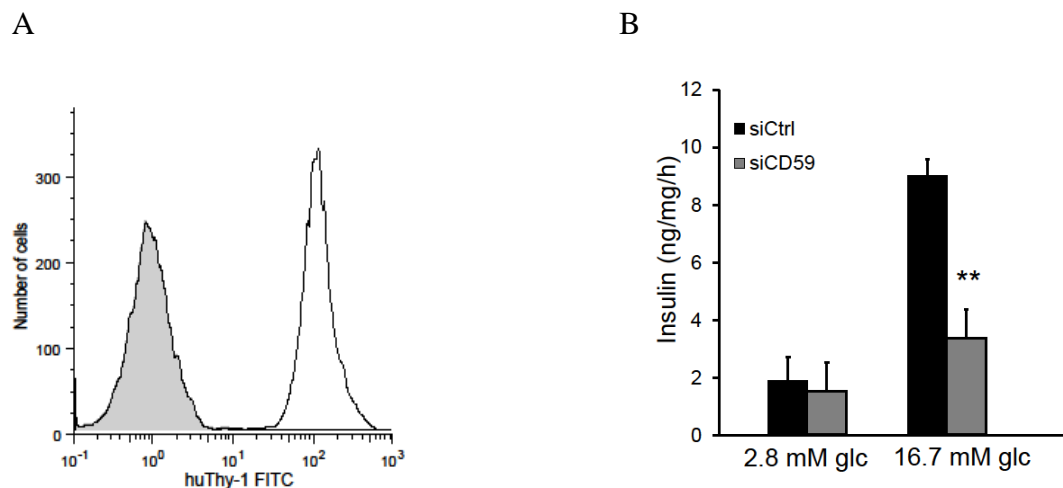
Figure S3: Overexpression of the GPI-linked protein Thy-1 in INS-1 832/13 cells does not affect insulin secretion, related to figure 3

(A) The open reading frame for human Thy-1 was cloned into the expression vector pKEVIN and INS-1 832/13 cells were transfected with pKEVIN-huThy1 using Lipofectamine 2000. INS-1 832/13 cells transfected with pKEVIN-huThy1 (black line) or empty vector (filled histogram) were stained with FITC-labeled anti-huThy-1 and expression assessed by flow cytometry. (B) To verify that pKEVIN itself had no effect on insulin secretion, we performed insulin secretion after siRNA silencing of CD59 in INS- 832/13 cells transfected with the empty control vector; n = 3, **P < 0.01.

A

2.8 mM glc   16.7 mM glc

siCtrl

siCD59

B

CD59 + flotillin

2.8 mM glc   16.7 mM glc

C

4
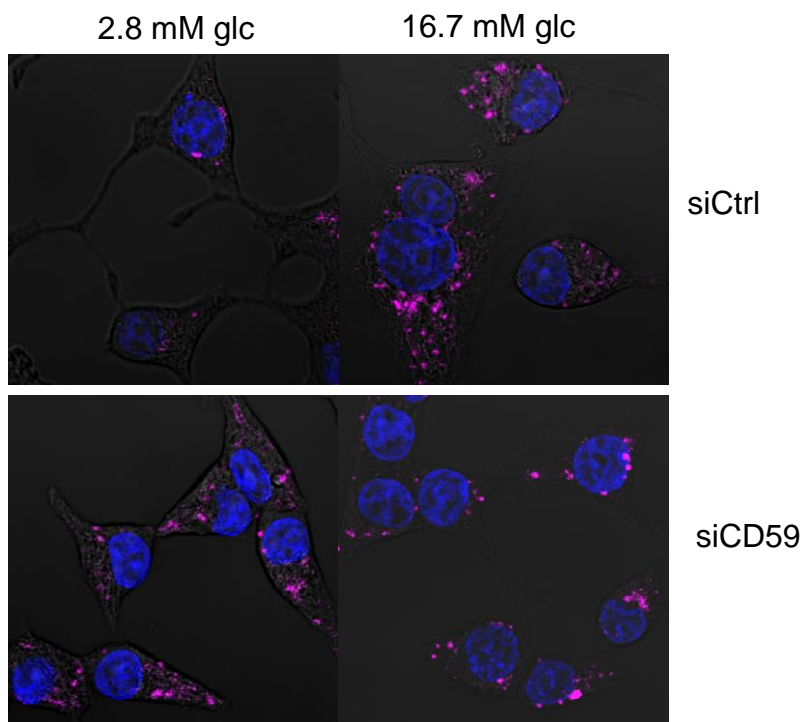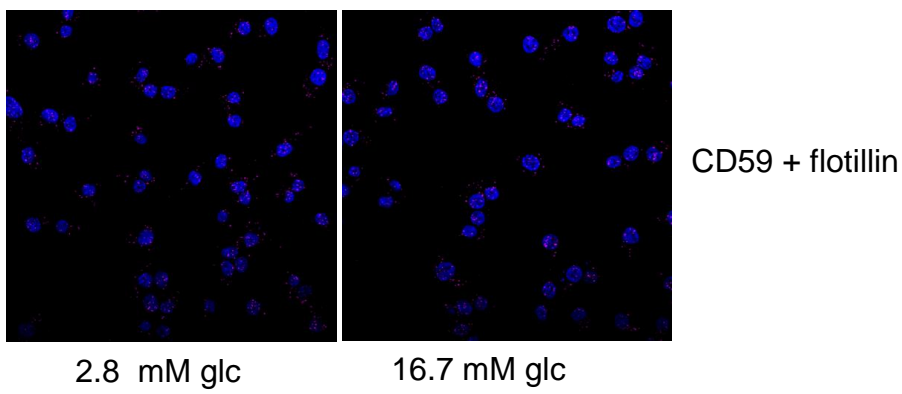
Figure S4: CD59 is required for glucose- and K^{+}-dependent colocalisation between VAMP2 and Syntaxin1A, related to figure 4

(A) Colocalization of VAMP 2 and Syntaxin1A. The colocalization was assessed using Olink PLA probes in cells in which CD59 was silenced as well as co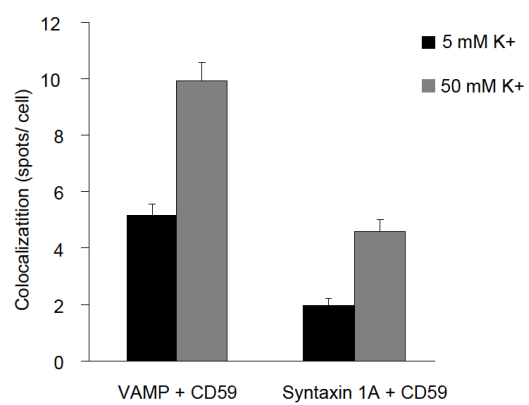ntrol cells. A fluorescent dot is generated when two antibodies are closer than 40 nm. (B) Colocalization of CD59 and the lipid raft marker flotillin in INS-1 832/13 cells does not increase by elevating glucose concentrations from 2.8 mM to 16.7 mM. (C) Colocalization of CD59 and VAMP2 as well as CD59 and Syntaxin1A increases when stimulated with high concentrations of K^{+}. Values represent means and SEM of 35 cells per condition.

SUPPLEMENTAL METHODS

Animals

Wistar and GK male rats (Charles River Laboratories, Wilmington, MA) 6-11 week of age was used. Blood glucose at termination was 7.1 ±1.3 mM for Wistar and 11.5± 2.3 mM for GK. Normoglycemic diabetes prone and diabetes resistant female BB rats (CRC, Malmö) ages approximately 40 days were used. The diabetes prone rats all develop T1D around 60 days. The rats were euthanized by CO$_2$.

Adult Akita (*Ins2$^{+/-}$*) and WT (*Ins2$^{+/+}$*) male littermates (7-13 weeks of age) were used. Mice originally purchased from Jackson laboratories (Maine, stock number 003548) and bred at our facilities on a mixed C57Bl/6J and FVBN background (~94% and 6%, respectively). Akita mice were genotyped according to protocols provided by the Jackson Laboratories. Blood glucose was measured weekly in whole venous blood using Contour Next EZ meter (Bayer AB) in non-fasting mice. Akita mice had sustained hyperglycemia from 4 weeks of age, with >25 mM at termination vs. 8.3 ±1.1 mM of control WT mice. Mice were anaesthetized with ketamine hydrochloride and xylazine (i.p.; 2.5 mg and 7.5 mg/100 g body weight, respectively) and euthanized by exsanguination.

Quantitative PCR

RNA was extracted using RNEasy (Qiagen). Gene expression was measured by QPCR using TaqMan (Applied Biosystems). RNA (0.5 µg) was used for cDNA synthesis with SuperScript (Invitrogen). The reaction mixture (5 µl), with 42 ng cDNA, 2.5 µl of TaqMan mastermix (Applied Biosystems), 1.25 µl of TaqMan gene expression assay, containing 900 µM primer, was analyzed in a 7900HT Fast Real-Time System (Applied Biosystems). The amount of mRNA was calculated relative to the amount of HPRT (hypoxanthine–guanine phosphoribosyltransferase) mRNA in the same sample by the formula $X_0/R_0 = 2^{CtR-CtX}$, where X_0 is the original amount of mRNA for the gene of interest, R_0 is the original amount of HPRT mRNA, C$_t$R is the C$_t$ (cycle threshold) value for HPRT, and C$_t$X is the C$_t$ value for the gene of interest. Taqman assays used: Rn00563929_m1 CD59, Rn01527840_m1 Hprt1, Rn01752026_m1 Polr2a, Rn00434830_m1 Masp1, Rn01430864_m1 Cfp, Rn00583199_m1 C3ar1, Rn00586108_m1 C5r1, Rn01519903_m1 C1qa, Rn00709472_m1 Daf1, Mm00453149_m1 CD59a, Mm02525679_s1 CD59b, Mm0399_m1 Hprt.

Cell culture

INS-1 832/13 β-cells were cultured in RPMI 1640 medium containing 11.1 mM D-glucose and supplemented with 10% fetal bovine serum, 100 units/ml penicillin, 100 μg/ml streptomycin,10 mM Hepes, 2 mM glutamine, 1 mM sodium pyruvate and 50 μM 2-mercaptoethanol, at 37∘C in a humidified atmosphere containing 95% air and 5%CO2.

Immunohistochemistry

Wistar rats were sacrificed and the pancreas immediately removed and fixed in 4% PFA, embedded in paraffin and cut into 5-μm sections. After antigen retrieval, the staining was done using primary antibodies against glucagon (rabbit-raised, Eurodiagnostica), insulin (guinea pig-raised, Novo Nordisk,), CD59 (mouse-raised, Abcam) and fluorescently labeled secondary antibodies (1:300, Jackson Immuno Research Labs).

RNA interference

Clonal INS-1 832/13 cells, alphaTC1-6 cells or A549 cells (ATCC) grown in RPMI 1640 were seeded in 24 well plates (250-400 000 cells/well). siRNA was mixed with Dharmafect (Dharmacon) in Optimem (Life Technologies) without antibiotics, and incubated at room temperature for 20 min. The mixture was then added to the cell culture media in a total volume of 0.5 ml giving a final siRNA concentration of 30 nM. The cells were then cultured for 48 or 72 h at 37 °C in a humidified atmosphere containing 95% air and 5% CO2 before experiments were performed.

Flow cytometry

CD59 levels on clonal INS1 cells and red blood cells were assessed by incubation in 10 μg/ml monoclonal mouse anti-CD59 antibody (AbD serotec) for 15 minutes at room temperature, followed by washing and staining with 1:200 FITC-labeled goat anti-mouse $F(ab)_2$ (DAKO) for 20 minutes, followed by a final wash. Red blood cells were separated from leukocytes by density centrifugation of fresh rat blood collected in citrate anticoagulant, using Optiprep (Axis Shield), following manufacturer's instructions. Thy-1 expression was similarly assessed on transfected INS1 clones by incubation with FITC-labeled mouse anti-Thy-1 (Abcam). Intracellular staining of dispersed islets was carried out by first fixing cells using buffer A from the Fix&Perm kit (ADG Bioresearch), according to instructions, then incubating cells in in permeabilization buffer (PBS/0.5%BSA/0.5% Tween-20) for 15 minutes, room temperature. All subsequent stainings were carried out at 4°C in permeabilization buffer for 30 minutes. CD59 levels were assessed using antibodies described above, while insulin-positive cells were detected using guinea pig anti-insulin serum (Euro Proxima) followed by Cy5 labeled anti-guinea pig antibody, Control primary antibodies of mouse IgG1 and non-immune guinea pig serum were used. Cells were analysed using the Cyflow Space flow cytometer (Partec).

Insulin secretion

Following transfection with siRNA against CD59 or a negative control sequence, INS-1 832/13 β-cells were seeded in 24-well plates. When assayed, cells were kept in HBSS (Hepes-balanced salt solution; 114 mM NaCl, 4.7 mM KCl, 1.2 mM KH_2PO_4, 1.16 mM $MgSO_4$, 20 mM Hepes, 2.5 mM $CaCl_2$, 25.5 mM $NaHCO_3$ and 0.2% BSA, pH 7.2) supplemented with 2.8 mM glucose for 2 h at 37°C. Insulin secretion was then measured by static incubation of cells for 1 h in 1 ml of HBSS containing 2.8 or 16.7 mM glucose or 2.8 mM glucose combined with 10 mM α-ketoisocaproic acid (KIC) or 35 mM K^+. Insulin was measured by the Coat-a-Count kit (DPC).

TIRF

Cell culture

INS-1 832/13 cells were plated on coverslips coated with poly-D-lysine and immediately transfected with 30 nM siControl or siCD59 using Dharmafect. After 6 hours, the same cells were transfected with the granule marker Neuro pepdideY-EGFP. Cells were imaged 42 h after plating in solution containing 138 mM NaCl, 5.6 mM KCl, 1.2 mM $MgCl_2$, 2.6 mM $CaCl_2$, 10 mM D-glucose, 5 mM Hepes (pH 7.4 with NaOH), 200 μM diazoxide and 2 μM forskolin. Exocytosis was evoked by timed local application of high K^+ (75 mM KCl equimolarly replacing NaCl) for 1 min through a pressurized glass electrode, similar to those used for patch clamp experiments. All experiments were carried out with constant buffer perfusion at 32 °C.

TIRF Microscopy

Cells were imaged using a custom-built lens-type total internal reflection (TIRF) microscope based on an Axiovert 135 microscope with a 100x/1.45 objective (Carl Zeiss). Excitation was from a DPSS laser at 473 nm (Cobolt,), controlled with an acousto-optical tunable filter (AA-Opto) and using dicroic Di01-R488/561 (Semrock) and emission filter FF01-523/610 (Semrock). Scaling was 160 nm per pixel and exposure time 100 ms per frame at 10 frames/s.

Image analysis. Exocytosis events were found by eye. The moment of exocytosis was defined as the first significant change (2 SD) from the pre-exocytosis baseline. This definition applied to both types of event, with or without preceding flash. The decay time was then defined as the time from exocytosis until the signal reached less than one third of the amplitude of the event. Traces were read out as ΔF, defined as average fluorescence in a 0.5 μm circle minus the average fluorescence in a surrounding annulus of 0.8 μm.

Glucagon secretion

The mouse clonal alpha-cell line alphaTC1-6 was cultured in DMEM, 10% hi FBS, 15mM Hepes, 0.1mM non-essential amino acids, 1.5g/L NaHCO3, 2g/L glucose, 0.02% BSA and P/S. Glucagon secretion was performed as insulin secretion with the exceptions that 5 mM glucose was used for preincubation, and the stimulatory conditions were 5 mM glucose or 5 mM glucose and 70 mM K^+.

Staining of lipid rafts

siControl and siCD59 transfected INS1 832/13 or A549 cells were seeded on 35 mm dishes with a glass window. They were treated with the organic dye Atto647N-labeled sphingomyelin (Atto-SM, Atto-Tec) diluted 1:100 in HEPES +DMEM for 20 min on ice. The cells were washed and fluorescent images were obtained using a Zeiss LSM 510 Meta Confocal microscope. The fluorescence intensity of Atto-SM was quantified by ZEN software 2009. Rat islets were dispersed in a Ca^{2+} free buffer, and left to stick to the glass for 24 h before stained as above.

Expression of Thy-1 in INS1 832/13 cells

The open coding region of human Thy-1 was synthesised using codon optimisation to optimise rat expression levels (DNA 2.0), cloned into the pKEVIN expression vector, and transfected into INS1 832/13 cells using lipofectamine 2000. Transfected cells were plated onto tissue culture dishes and clones picked under hygromycin selection. Clones with high Thy-1 expression and comparable insulin secretion to wild type cells were used for CD59 knockdown experiments. Control cells were transfected with empty vector only.

Immunocytochemistry

Clonal INS-1 832/13 cells

INS-1 832/13 cells were cultured on glass cover slips for 18 h. Thereafter, cells were fixed with 150 μl 3% paraformaldehyde (PFA) in K-PIPES at pH 6.8 (Sigma) for 5 min at room temperature (RT) before a second fixation with 150 μl 3% PFA in NaB_4O_7 at pH 11 incubated 5 min at RT. Following washing with 200 μl PBS×2, the cells were permeabilised in 100 μl 0.1% Triton X-100 in PBS for 30 min. For unpermeabilized cells this step was omitted. Thereafter, the cells were washed once in PBS and incubated 15 min with 100 μl 5% normal donkey serum to avoid non-specific binding. The cells were then incubated with primary monoclonal mouse antibody against rat CD59 (NordicBioSite, AbD serotec) for 2 h at room temperature (1:25 and 1:50). The cells were then washed twice with 200 μl PBS, and incubated 10 min with 100 μl 5% NDS-PBS at RT, before incubation 1 h in the dark with the secondary antibody DyLight 649 donkey anti-mouse (Jackson Immuno Research Labs) for 1 h at room temperature (1:200). Next, the cells were washed three times with 200 μl PBS and post-fixed with 200 μl 3% PFA for 10 min at RT. Following three washings with 200 μl PBS, a final wash with 200 μl sterile-filtered mp-H_2O was performed. After drying, the cells were mounted onto object glass using mounting medium before confocal microscopy analysis.

Primary rat islet cells

Dispersed islets cells were seeded on glass cover slips and cultured for 24 h. The cells were then preincubated in 2.8 mM glucose for 1 h, and afterwards incubated at 2.8 or 16.7 mM glucose for 1 h. Thereafter the protocol for clonal cells was followed. Primary antibodies: Mouse anti-rat CD59, monoclonal (NordicBioSite, AbD serotec) 1:25, Guinea pig anti-insulin (Linco) 1:200. Secondary antibodies: DyLight 649 Donkey anti-mouse (Jackson Immuno

Research Labs), red 1:200, Cy 2, Donkey anti guinea pig (Jackson Immuno Research Labs), green 1:200.

Duolink *in situ* detection

INS-1 832/13 cells were transferred on the μ-8-well plate (iBidi) 12-24 h before staining experiments. The cells then were fixed by 3% PFA for 30 min and permeablized with Perm Buffer III (BD) for 40 min. The primary antibodies of anti-CD59 (NordicBioSite, AbD serotec), anti-VAMP2 (Abcam) and anti-syntaxin1A (Synaptic Systems) were diluted by 1:50, 1:5000 and 1:200 respectively and incubated with cells overnight. Continuous staining protocol followed the instruction from Olink Bioscience. Briefly, PLA probes of 20 μl anti-rabbit Plus and 20 μl anti mouse Minus were diluted in 60 μl blocking buffer and incubated with cells for 1h in 37C. The ligation buffer (1:100 dilution of ligase) added into cells for 30 min in 37C. The amplification buffer (1:100 dilution of polymerase) was added to cells after washing. Finally the cell nuclei were stained by Hoechst 23458 (Invitrogen). The spots were imaged by confocal microscopy and the spot numbers per cell were calculated by Duolink Image Tool (Olink Bioscience).

ELISA

INS-1 cells were grown in 8 separate flasks and upon confluency incubated for 24h in low (2.8 mM) and high (16.7 mM) glucose medium and lysed with PBS supplemented with 10 mM EDTA, 1 mM PMSF and 1% Triton X-100. Lysates were centrifuged at 10 000 g for 3 min and the supernatants diluted to 40% in lysis buffer were added to microtiter plates coated with 0.5 μg/ml of antibodies against VAMP2 (Synaptic Systems), Syntaxin1A (Synaptic Systems) or isotype control antibodies (Immunotools) and blocked with 3% fish gelatin in washing buffer (50 mM Tris-HCl, 150 mM NaCl, 0.1% Tween 20 pH 7.5). After 1h incubation at 37°C the plates were washed and incubated with biotinylated antibodies against rat CD59 (mAb TH9, Hycult). After 1h incubation, the plates were washed and incubated with streptavidin-HRP (R&D) for 1h followed by development with 1,2-phenylenediamine dihydrochloride (OPD)-tablets according to manufacturer's instructions (Dako). The absorbance at 490 nm was measured with Cary 50 MPR microplate reader (Varian). Weak, unspecific signal obtained with isotype control antibodies was subtracted.

Immunoprecipitation

INS1 832/13 cells (5×10^6) were incubated in RPMI 1640 medium with 16.7 mM glucose for 24 h. Next cells were washed with PBS and harvested in 0.5 ml of lysis buffer (50 mM Tris-HCl pH 7.5; 150 mM NaCl; 0.2% Triton X-100; 0.2% NP-40; 1mM EGTA; protease inhibitors (Roche Diagnostic Corporation)). Lysate was spun at 10 000 x g in 4°C and obtained supernatant was subjected BCA (ThermoFisher Scientific) protein quantification assay. Sample of lysate was saved as 'Input' (30 μg). The rest of lysate (~450 μl) was mixed with 10 μg antibodies - anti-syntaxin1A (Synaptic Systems) or IgG1 (ImmunoTools,) covalently bound to 2 mg of magnetic DynaBeads® (Life Technologies) and incubated on the roller shaker over-night in 4°C. Next beads were extensively washed with lysis buffer and co-precipitated proteins eluted with 150 μl of elution buffer (Glycine-HCl, pH 3). Samples were

run in Laemmli set-up in non-denaturing conditions. Briefly, 15 µg of protein samples were loaded on 15% polyacrylamide gel, proteins separated, transferred onto PVDV membrane, blocked with 5% milk in TBST buffer and probed with 1: 500 dilution of anti-syntaxin1A, anti-VAMP2 (Synaptic Systems), 1:200 of anti-CD59 and 1:1000 of anti-beta-actin (Sigma) antibodies. The membranes were incubated with 1:1000 dilution of anti-mouse horseradish peroxidase coupled secondary antibodies and signal was obtained owing to SuperSignal West Pico Chemiluminescent Substrate (ThermoFisher Scientific).